Quaternary stratigraphy of Bayan Borehole in eastern Songnen Plain and its Palaeoclimate Significance

Haonan Song
China Geological Survey
Zhongkai Liang
China Geological Survey
Mingxin Duan
China Geological Survey
Muxiao Liu
Yunnan University
Liye Liu
China Geological Survey
Zhuo Chen
China Geological Survey
Shoude Han
China Geological Survey
Haicheng Zhang
China Geological Survey
Chuanfang Zhou
zhouchuanfang@mail.cgs.gov.cn
China Geological Survey

Article

Keywords: Songnen Plain, Quaternary, Magnetic stratigraphy, Grain-size end-member, Palaeoclimate

Posted Date: May 23rd, 2025

DOI: https://doi.org/10.21203/rs.3.rs-6459786/v1

Additional Declarations: No competing interests reported.

Version of Record: A version of this preprint was published at Scientific Reports on August 31st, 2025. See the published version at https://doi.org/10.1038/s41598-025-15418-6.

Abstract

The Songnen Plain is a key region for Quaternary stratigraphic research in Northeast China. In this area, the Quaternary strata of the Bayan borehole reached a thickness of 58.00 m, offering excellent potential for detailed investigation. A comprehensive analysis of the borehole was conducted using lithological characteristics, optically stimulated luminescence (OSL), electron spin resonance (ESR), magnetic susceptibility, grain-size distribution, and magnetostratigraphy. Based on these results, a polarity stratigraphic framework was established, subdividing the sequence into four units: the Holocene Series (0–1.50 m), Guxiangtun Formation (1.50–18.80 m), Harbin Formation (18.80–35.50 m), and Huangshan Formation (35.50–58.00 m). Chronostratigraphic and paleoenvironmental interpretations were derived to establish a Quaternary stratigraphic framework for the eastern Songnen Plain. Grain-size end-member analysis was applied to the Bayan borehole using the Analysize method to extract three effective grain-size components. EM_1 (6.72 μm) corresponded to the atmospheric background dust; EM_2 (21.20 μm) reflected the input from distal dust sources associated with summer monsoon signals; and EM_3 (45.60 μm) indicated the proximal deposition influenced by winter monsoon intensity. Comparative analysis of magnetic susceptibility, M_z, grain-size end-members, and marine isotope stages revealed strong correlations, identifying multiple climate response events. In the eastern Songnen Plain, the Middle Pleistocene was marked by a transition from dry-cold to cool-moist conditions, with a boundary at approximately 250 ka. During the Late Pleistocene, the region experienced alternating phases of dry-cold and cool-semi-humid conditions. The Holocene was characterized by a warm and semi-humid climate. These findings provide a robust data foundation for refining the Quaternary stratigraphy of the Songnen Plain and offer critical insights into regional paleoclimatic evolution.

1. Introducation

The Songnen Plain is a key region for Quaternary stratigraphic research in Northeast China and represents one of the most significant areas for loess development, attracting growing scholarly attention in recent years [1–21]. Previous research on Quaternary loess in the eastern Songnen Plain has primarily concentrated on the Huangshan section near Harbin, which serves as a representative and well-studied section [4,9,10,14–18,22]. Detailed investigations have addressed its stratigraphic framework, lithological features, genesis, and paleoenvironmental implications. However, comprehensive Quaternary studies beyond the Huangshan section remain limited. Most existing research is site-specific and lacks regional stratigraphic correlations and broader multi-site data support. As a result, high-resolution analyses of sedimentary provenance and paleoclimatic evolution across the eastern Songnen Plain remain insufficient. With recent advancements in subsurface geological investigations [23–27], the volume of Quaternary stratigraphic data has significantly increased, progressively addressing these regional knowledge gaps [19–21]. Extensive fieldwork has revealed that the Bayan borehole situated north of the Huangshan section contains a notably thick Quaternary sequence, underscoring its strong potential for future stratigraphic and paleoenvironmental studies.

This study presented high-resolution grain size and magnetostratigraphic analyses of representative Quaternary borehole from the Bayan area. Integrated with chronological data, this study established a detailed stratigraphic framework and enabled a regional stratigraphic correlation. By reconstructing the depositional environments and analyzing the variations in grain-size end-members, this study further elucidated the paleoclimatic evolution of the region since the Middle Pleistocene. These findings could provide critical insights into the development of the Quaternary system in the Songnen Plain and contribute to a deeper understanding of the regional paleoclimate dynamics.

2. General Overview of the Study Area and Lithological Characteristics

2.1 General Overview of the Study Area

Bayan County, located in the eastern part of the Songnen Plain and northwest of Harbin City, is geographically positioned with the mainstream of the Songhua River to the south, low-rolling hills to the east, Hulan District to the west along the Piao River, and Suihua City to the north across the Ni River. The region experiences a temperate semi-humid to semi-arid continental monsoon climate characterized by cold winters, hot summers, and frequent strong winds, which are highly favorable for dust deposition and accumulation.

The study area is geomorphologically situated on the second terrace of the Songhua River and represents a typical loess accumulation zone within the Songnen Plain. The Quaternary strata are primarily composed of the Tantu Formation (Holocene), Guxiangtun Formation (Upper Pleistocene), Harbin Formation (Middle Pleistocene), and Huangshan Formation (Middle Pleistocene) [28]. Geologically, the area lies on the eastern margin of the Songliao Rift Basin (K-N) and the southeastern margin of the Xiao Hinggan Mountains-Zhangguangcai Mountains arc-basin transitional zone. It is located north of the Songhua River reverse fault and has undergone continuous erosion and uplift due to compressional thrusting of the Songhua River fault and adjacent mountain ranges [29]. Influenced by neotectonic activity and freeze-thaw processes, the region exhibits widespread gully development, forming a landscape of extensive plains interspersed with gently undulating hills [3].

2.2 Lithological Characteristics

The Bayan borehole is situated south of Ping'an Village, Fengle Township, Bayan County, Harbin City (46°14'0.80"N, 127°04'5.87"E; elevation: 184.00 m), approximately 104 km from Harbin, with a total drilling depth of 93.75 m (Fig. 1). The Quaternary loess sequence extends from 0 to 56.55 m and is primarily composed of yellowish-brown clay and sandy soil. The upper portion exhibits a granular structure, while the rest sections transition into a blocky structure with moderate compaction, weak luster, and sporadic occurrences of calcareous nodules and ferruginous staining. Between 56.55

and 90.55 m, the strata consist of grayish-white gravelly sand, displaying a sandy-gravelly texture, loose fabric, rough fracture surfaces, and faint luster. Gravel ranges from 2 to 8 mm in diameter and is abundant, likely representing fluvial bar or oxbow lake deposits. From 90.55 to 93.75 m, bluish-gray semi-consolidated fine sandstone appears, featuring a sandy structure, relative hardness, and minor gravel content, suggesting a transition into the upper Nenjiang Formation, characterized by fluvial deposition. This study primarily focused on Quaternary strata from 0 to 58.00 m depth (Fig. 2).

3. Sample Collection and Testing

To determine the chronological framework of the strata, four optically stimulated luminescence (OSL) and two electron spin resonance (ESR) samples were collected at various core intervals. Sampling was performed using steel tubes with a diameter of 10 cm, which were driven into the target layers immediately after drilling, prior to core hardening. The ends of the tubes were sealed with wooden plugs and wrapped in opaque plastic bags to prevent light exposure. All samples were sent to the Qingdao Institute of Marine Geology, China Geological Survey for analysis. OSL dating was performed using a CANBERRA-BE3830 high-purity germanium γ-spectrometer and a LEXSYG research-grade luminescence reader under controlled laboratory conditions (23–25°C and 30–50% relative humidity). ESR dating employed a Bruker EMXplus ESR spectrometer in conjunction with the same γ-spectrometer, with measurements conducted at 20–25°C and 20–50% relative humidity.

Granulometric analysis was performed on 485 sediment samples collected at 10 cm intervals from core depths between 0.00 and 48.50 m. In the laboratory, organic matter was removed using 10 mL of 30% H_2O_2, followed by addition of 10 mL of 10% HCl to eliminate carbonates. After rinsing with distilled water and centrifugation, a 10 mL aliquot of 0.05 mol/L sodium hexametaphosphate ($(NaPO_3)_6$) was added as a dispersant, and the samples were dispersed by oscillation. Distilled water was added again before measurement. The particle size distribution was determined using a Mastersizer 3000 laser diffraction granulometer with a measurement range of 0.02–2000 μm and a repeatability error of less than 0.2%. All analyses were conducted at the Key Laboratory of Cold Region Geography Environment Monitoring and Spatial Information Service at Harbin Normal University.

Susceptibility samples were collected at regular intervals from core depths between 0.60 and 51.85 m, yielding a total of 200 specimens. Sampling was performed using non-magnetic plastic cubic boxes, each measuring 2 cm × 2 cm × 2 cm. Measurements were performed at the Experimental Testing Center of the Qingdao Institute of Marine Geology, China Geological Survey. A Bartington Susceptibility Meter was employed for the analysis, with the testing conditions maintained at 20–22℃ and relative humidity controlled between 39% and 40%.

Paleomagnetic samples were collected at 10 cm intervals from core depths of 30.00 to 58.90 m, yielding 290 specimens. Sampling was conducted using non-magnetic orientation-preserved plastic cubic boxes (2 cm × 2 cm × 2 cm). The remanent magnetization was measured using a 2G-760 three-axis horizontal superconducting magnetometer in a magnetically shielded environment (residual field < 300 nT). All samples underwent the stepwise alternating field demagnetization in 15 steps: NRM, followed by 2.5, 5, 7.5, 10, 12.5, 15, 17.5, 20, 30, 40, 50, 60, 80, and 90 mT. Paleomagnetic analyses were performed at the Key Laboratory of Paleomagnetism and Paleotectonic Reconstruction, Ministry of Natural Resources.

4. Results

4.1 OSL and ESR

The results of age determination are presented in Table 1. According to the dating data, the sedimentation age at a depth of 17.8 m in the Bayan borehole was 40.8 ± 2.1 ka, suggesting that the 0–17.8 m interval corresponded approximately to the middle and upper sections of the Guxiangtun Formation. The age at the 50.8 m depth was 420.91 ka, indicating that the lower portion of the borehole was likely attributable to the Huangshan Formation.

Table 1
Statistics of OSL and ESR dating results.

Number	Sample depth/m	U/×10^{-6}	Th/×10^{-6}	K/%	Water content/%	Dose rate/ (Gy/ka)	ka
SHOSL-01	1.5 ~ 1.7	1.91	8.02	1.72	24.70	29.00	10.5 ± 1.0
SHOSL-02	5.0 ~ 5.2	2.38	10.79	1.88	20.67	71.37	21.5 ± 0.3
SHOSL-03	10.8 ~ 11.0	1.39	7.41	1.75	14.73	92.03	33.5 ± 7.9
SHOSL-04	17.6 ~ 17.8	2.23	9.50	1.88	16.01	132.42	40.8 ± 2.1
SHESR-01	37.9 ~ 38.1	7.49	13.75	2.91	7.71	5.64	255.15
SHESR-02	50.6 ~ 50.8	4.50	14.64	2.40	21.19	3.91	420.91

4.2 Grain size

In this study, widely accepted boundary values of 63, 16, and 4 μm were used to classify the sand, coarse silt, fine silt, and clay fractions, respectively [10,11,15–17]. The grain size analysis results (Fig. 3) show that sand (> 63 μm) comprises 0.00–51.70% of the samples, with an average of 6.74%. Coarse silt (16–63 μm) ranged from 10.86–62.09%, averaging 42.68%, and represented the primary modal grain-size component. Fine silt (4–16 μm) accounted for 11.33–66.64%, with a mean of 38.99%, serving as the secondary modal group. The clay (< 4 μm) ranged from 2.78–36.68%, with an average of 11.58%.

The grain-size parameters were calculated using the formula proposed by Folk and Ward [31]. The results (Fig. 3, 4) showed that the median grain size (M_d) ranged from 3.90 to 7.42 φ, with a mean value of 5.95 φ. M_z varied from 4.06 to 7.79 φ, averaging 6.05 φ. The standard deviation (σ) indicating sorting ranged between 0.99 and 1.96, with an average of 1.49. *Sk* varied from − 0.47 to 0.05, with a mean of − 0.16. K_G ranged from 0.84 to 1.47, with an average of 1.04.

4.3 Magnetic susceptibility

The magnetic susceptibility of the Bayan borehole displayed a distinct pattern of periodic fluctuations. The mass-specific susceptibility ranged from 3.69–25.11×10^{-8} m^3/kg, with an average value of 9.25×10^{-8} m^3/kg. Previous studies in the region reported that the magnetic susceptibility of the Huangshan loess near Harbin varied between 8.3 and 94.7 × 10^{-8} m^3/kg, with a mean of 32.3 × 10^{-8} m^3/kg [16]. Similarly, the Huangshan core exhibited the periodic high and low values, ranging from 4.01 to 94.69 × 10^{-8} m^3/kg, with an average of 29.07 ×10^{-8} m^3/kg [15]. When compared with the magnetic susceptibility curves from the Huangshan section of the eastern Songnen Plain, several consistent trends and correlations were observed (Fig. 5).

4.4 Establishment of Paleomagnetic and Magnetic Stratigraphic Sequences

Paleomagnetic samples from the Bayan borehole were analyzed using orthogonal projection diagrams to interpret the demagnetization results. The principal vector directions were determined using the least-squares method [32], and the remanence directions were calculated using PaleoMag software. The representative orthogonal projections of alternating field demagnetization for the selected samples are presented in Fig. 6. The natural remanent magnetization (NRM) intensity ranged from approximately 10^{-5} to 10^{-6} A/m. The low-coercivity components were generally removed between 15 and 20 mT, allowing for the isolation of the high-coercivity components, which were defined as the characteristic remanent magnetization (ChRM). In most cases, stable ChRM directions were identified within the 40–80 mT demagnetization window. Based on the criterion of a maximum angular deviation (MAD) less than 16°, 102 samples yielded stable ChRM directions, representing 35.17% of the total samples analyzed.

Following the principle that three or more consecutive samples with consistent polarity define a single polarity zone and considering the potential randomness in magnetic declination of borehole samples, only magnetic inclination data were adopted to construct the magnetostratigraphic polarity sequence of the Bayan borehole (Fig. 7). The resulting polarity sequence was correlated with the geomagnetic polarity time scale (GPTS)[33–37], combined with the ESR age data. The Bayan borehole preserved one long normal polarity zone (N1) spanning 30.00–58.00 m and three geomagnetic excursion events: excursion e_1 (30.90–32.40 m), excursion e_2 (37.40–38.20 m), and excursion e_3 (53.20–54.40 m). The normal polarity zone N1 corresponded to Brunhes Chron, while the three negative excursions were interpreted as the Iceland Basin, Calabrian Ridge 0, and an unnamed geomagnetic excursion, respectively.

5. Analysis and Discussion

5.1 Division and Discussion of the Epochs in the Quaternary Stratigraphy

Based on the OSL and ESR dating, the age at 1.50 m was 10.5 ± 1.0 ka, which fell within the Holocene epoch, as the boundary between the Holocene and Pleistocene was defined at 11.7 ka [38]. The sediment (0–1.50 m) was composed of gray-black silt loam with a granular structure and occasional ferruginous-manganese concretions. Therefore, this section of the Bayan borehole was assigned to the Holocene Series.

Based on the age data, the sedimentary age of the 1.50–17.80 m interval in the Bayan borehole ranged from 10.5 ± 1.0 to 40.8 ± 2.1 ka, corresponding approximately to the upper part of the Guxiangtun Formation. The 1.50–5.65 m section consisted of gray-brown sandy loam with a granular structure, moderate compaction, occasional iron-manganese nodules, and observable horizontal bedding. Between 5.65–17.80 m, the deposits comprised soil-yellow to brownish-yellow clayey silt and sandy clay with scattered black carbon fragments and calcareous nodules, showing both cross-bedding and horizontal bedding. From 17.80–18.80 m, the layer was composed of black clay rich in iron-manganese nodules, likely representing a paleosol horizon. Previous studies divided the Guxiangtun Formation into two segments: an upper unit of gray-black subclay and light yellow loess-like soil interbedded with paleosols, and a lower unit of clayey silt and clay [14,28]. Ye [39] proposed a lower boundary age of 100 ka for the Guxiangtun Formation, while the Bureau of Geology and Mineral Resources of Heilongjiang Province [29] suggested a broader range of 1–70 ka. In contrast, Wang et al. [14] estimated the formation's age to be 12–79 ka. The magnetostratigraphic analysis identified the e_1 geomagnetic excursion at 30.90–32.40 m as corresponding to the Iceland Basin excursion, dated to 188 ka [34–36,40]. Using this reference point, an upward sedimentation rate calculation suggested that the depositional age at 18.80 m generally coincided with the lower boundary of the Guxiangtun Formation, as previously

proposed [14,29]. Based on an integrated analysis of chronological data, lithological features, and magnetostratigraphy, the strata between 1.50 and 18.80 m in the Bayan borehole were attributed to the Guxiangtun Formation, with a depositional age corresponding to the middle to late Late Pleistocene.

The 18.80–35.50 m interval of the Bayan borehole was composed of yellow-brown to earth-yellow silty sand with a relatively compact texture, containing calcareous particles and iron-manganese concretions. The typical lithology of the Harbin Formation includes light yellow to brown-yellow silts, with loess-like sandy silt near the top, often containing calcareous and iron-manganese nodules and iron-stained bands [29]. Previous studies have dated the Harbin Formation to 79–138 ka, corresponding primarily to the early Late Pleistocene [14], while Wang [8] estimated its depositional age to be 136–200 ka based on Quaternary sedimentary sequences in the Harbin area. The Regional Geology of Heilongjiang Province [29] assigned the Harbin Formation to the late Middle Pleistocene–early Late Pleistocene. In the Bayan borehole, the ESR dating yielded an age of 255.15 ka at a depth of 37.90 m. Additionally, the e_2 geomagnetic excursion (37.40–38.20 m) corresponded to the Calabrian Ridge 0 excursion, dated to approximately 260 ka [33–35]. These ages were older than the conventionally accepted lower boundary of the Harbin Formation. Considering the combined evidence from ESR and magnetostratigraphy, along with lithological characteristics, the 18.80–35.50 m interval in the Bayan borehole was assigned to the Harbin Formation, with a depositional age ranging from the late Middle Pleistocene to the early Late Pleistocene.

The 35.50–39.75 m interval of the Bayan borehole consisted of gray-brown silty clay, compact in texture with occasional rust-colored mottling and a smooth tactile quality. From 39.75–45.45 m, the lithology transitioned to slightly consolidated yellow-brown sandy clay exhibiting calcification, iron-manganese concretions, and clear stratification. Between 45.45–49.00 m, gray-black to gray-yellow clay was present, featuring well-defined stratification, limonite mineralization, and calcareous inclusions. From 49.00–58.00 m, the upper portion (~ 2 m) was composed of brown silt with occasional ferruginous concretions, while the remainder was yellow-brown gravelly fine sand with rust staining and a loose structure. The strata from 35.50 to 58.00 m in the Bayan borehole exhibited a progressive darkening in color and a lithological transition from fine clay and sandy soils to gravelly fine sand, which was indicative of fluvio-lacustrine sedimentary environments. Historically, researchers have subdivided the Huangshan Formation into two units: Upper Huangshan and Lower Huangshan [8,14,28,29]. The lithology of the Upper Huangshan Formation consisted of yellow-brown, brown-yellow, gray, and dark gray silty clay, with the upper section composed of loose gravelly sandy soil. In contrast, the Lower Huangshan Formation was characterized by yellow-green to gray-yellow silty clay, muddy silty sand, medium-to-coarse sand, and gravelly medium-fine sand. The Upper Huangshan can be dated to 200–400 ka, corresponding to the Middle Pleistocene, while the Lower Huangshan ranges from 400 to 700 ka, aligning with the early Middle Pleistocene [8,29]. The ESR and paleomagnetic data from the Bayan borehole yield an ESR age of 420.91 ka at a depth of 50.60 m. Additionally, the e_3 geomagnetic excursion identified between 53.20 and 54.40 m corresponded to the unnamed geomagnetic excursion dated at 400–420 ka [33,34]. Both dates fell within the time frame of the Lower Huangshan Formation. Given the integrated analysis of chronology, lithological characteristics, and magnetostratigraphy, this study did not further subdivide the formation because of the difficulty in accurately distinguishing the boundary between the Upper and Lower Huangshan Formations. The strata between 35.50 and 58.00 m in the Bayan borehole were assigned to the Huangshan Formation, with a depositional age corresponding to the middle Middle Pleistocene (Fig. 8).

The Bayan borehole is situated on the eastern clayey ridge high plain of Songnen Plain. This region exhibits ridge-like undulations shaped by fluvial erosion and denudation, forming a pediment erosion surface alongside episodes of riverine deposition [29]. During the Middle Pleistocene, the eastern high plain underwent regional uplift, leading to gradual shrinkage of the ancient Songnen Lake [10] and deposition of the Huangshan Formation in a shallow lacustrine setting. In the late Middle Pleistocene, the region experienced relatively stable subsidence, allowing for sustained loess accumulation and the onset of Harbin Formation deposition. During the early to middle stages of the Late Pleistocene, the eastern high plain of the Songnen Plain began to experience uplift, elevating the secondary lacustrine terraces above the water level. Influenced by neotectonic activity, intensified crustal uplift and fluvial downcutting led to the formation of relatively elevated river terraces [8,15,17,19]. These terraces subsequently underwent river deposition, giving rise to the Guxiangtun Formation.

5.2 Discussion on Grain Size Characteristics and Genesis of Quaternary Stratigraphy

The grain-size characteristics of Quaternary sediments can provide a direct reflection of sediment transport dynamics and depositional environments. Systematic, high-resolution grain-size analysis is an effective tool for interpreting sedimentary processes and genesis [6,41–44]. Because of the relatively thin Holocene strata and the limited number of grain-size samples in the Bayan borehole, attributable to its more recent deposition, this section is excluded from further discussion.

Table 2
Statistics of Grain size composition and parameters of Quaternary strata in Bayan borehole.

Formation	depth/m	Clay < 4 μm		Fine silt 4 ~ 16μm		Coarse silt 16 ~ 63 μm		Sand > 63 μm	
		Average	Range	Average	Range	Average	Range	Average	Range
Guxiangtun	1.50 ~ 18.80	9.45%	2.78%~29.84%	31.41%	11.33%~59.30%	42.47%	10.86%~62.09%	11.66%	0.00%~51.70%
Harbin	18.80 ~ 35.50	11.93%	2.99%~36.68%	42.86%	16.40%~61.27%	41.30%	14.67%~59.04%	3.90%	0.00%~24.86%
Huangshan	35.50 ~ 58.00	14.20%	5.26%~24.04%	44.97%	26.79%~66.64%	37.54%	12.43%~49.82%	3.29%	0.00%~14.87%
		M_d/μm		M_z/μm		*Sk*		K_G	
		Average	Range	Average	Range	Average	Range	Average	Range
Guxiangtun	1.50 ~ 18.80	22.69	6.26 ~ 47.30	28.75	7.42 ~ 65.77	-0.19	-0.46 ~ 0.01	1.03	0.84 ~ 1.36
Harbin	18.80 ~ 35.50	14.95	5.83 ~ 35.80	18.54	7.39 ~ 42.33	-0.15	-0.29 ~ 0.03	1.05	0.87 ~ 1.47
Huangshan	35.50 ~ 58.00	13.08	6.93 ~ 23.70	17.00	8.16 ~ 29.77	-0.13	-0.26 ~ 0.05	1.04	0.86 ~ 1.46

5.2.1 Discussion on Grain Size Characteristics and Genesis of the Guxiangtun Formation

The sedimentary interval from 1.50 to 18.80 m in the Bayan borehole is assigned to the Guxiangtun Formation, corresponding to the middle-late Late Pleistocene. The grain-size composition and parameter characteristics are listed in Table 2. The average proportion of coarse silt (16–63 μm) was 42.47%, representing the dominant modal grain size group, whereas fine silt (4–16 μm) constituted the secondary modal component, with an average content of 31.41%. The M_d ranges from 6.26 to 47.30 μm, averaging 22.69 μm, and M_z varies from 7.42 to 65.77 μm, with an average of 28.75 μm. The average standard deviation (σ) is 1.54. Based on the mixed sediment classification scheme [45,46], most samples plotted within the silt field on the lithological triangle diagram, with fewer samples classified as clayey silt. The grain-size frequency curves display a single broad peak, a weak secondary peak in the finer fraction, and exhibit negative skewness (Fig. 9).

The M_d of the Guxiangtun Formation is clearly reflected in its grain-size frequency curves, indicating a high-energy transport environment. The average standard deviation of 1.54 suggests poor sorting. The C-M plot positions the samples within the transition from graded suspension to uniform suspension, implying a transport regime capable of carrying coarser particles. The graded suspension deposits are characterized by a proportional increase in both C and M values; as bottom current velocity decreases, uniform suspension transitions into graded suspension, leading to sediment deposition. This pattern is typical of fluvial sediments in modern depositional basins [47–50]. Based on the combined analysis of the grain-size parameters and lithological features from the core, the Guxiangtun Formation is interpreted to have formed in a fluvial depositional environment.

5.2.2 Discussion on Grain Size Characteristics and Genesis of the Harbin Formation

The strata from 18.80 to 35.50 m in the Bayan borehole were assigned to the Harbin Formation, with a sedimentary age ranging from the late Middle Pleistocene to the early Late Pleistocene. The grain-size composition and parameter characteristics are listed in Table 2. The fine silt fraction (4–16 μm) averaged 42.86%, constituting the dominant modal grain size group, whereas the coarse silt fraction (16–63 μm) averaged 41.30%, forming the secondary group. M_d was 14.95 μm, and M_z was 18.54 μm. Compared to the Guxiangtun Formation, the Harbin Formation exhibits significantly finer particles, with silt content reaching up to 84.16%, indicative of reduced transport energy and finer sediment sources. Previous studies have demonstrated that the coarse silt fraction constitutes the “aeolian basic grain group”, forming the primary component of typical aeolian loess, while the clay fraction represents the “entrained grain group”, serving as a secondary modal grain size group [41]. This grain-size distribution reflects the atmospheric background conditions of aeolian loess regions and indicates a sustained process of dust deposition [9]. Aeolian loess sediments are generally poorly sorted, with suspended particles smaller than 70 μm dominating their composition [51]. The grain-size composition of the Harbin Formation supports the aeolian deposition theory. The grain-size frequency curve exhibited a broad secondary peak near 1 μm, reflecting the clay fraction linked to atmospheric background processes. The curve demonstrated a bimodal distribution, weak negative skewness, and a relatively sharp primary peak (Fig. 10a). Most grain-size samples fell within the clayey silt category, with occasional occurrences in the sandy clay and sand-silt-clay zones (Fig. 10b). The C-M diagram (Fig. 10c) suggests that the samples were situated in the transitional zone between uniform suspension and pelagic suspension, with a distribution trend parallel to the C = M line. This indicated the predominance of finer particles and a lower transport energy relative to fluvial processes, which is consistent with previous studies [9,10,15]. These characteristics collectively indicated that the Harbin Formation was deposited in an aeolian environment.

5.2.3 Discussion on Grain Size Characteristics and Genesis of the Huangshan Formation

The strata from 35.50 to 58.00 m in the Bayan borehole were assigned to the Huangshan Formation, with a sedimentary age corresponding to the mid Middle Pleistocene. The grain-size composition and parameter characteristics are detailed in Table 2. The very fine silt fraction (4–16 μm) averaged 44.97%, representing the dominant modal grain size group, whereas the coarse silt fraction (16–63 μm) averaged 37.54%, serving as the secondary modal group. The M_d ranged from 6.93 to 23.70 μm, with an average of 13.08 μm, and the M_z ranged from 8.16 to 29.77 μm, averaging 17.00 μm. The grain-size frequency curve was characterized by a distinct single peak, a weak secondary peak in the finer fraction, and negative skewness (Fig. 11a), similar to the pattern observed in the Guxiangtun Formation. However, both the median and mean grain sizes were notably finer than those of the Guxiangtun Formation. In the ternary lithology plot, most samples fell within the silty clay domain, with a smaller number located in the sand-silt-clay transitional zone (Fig. 11b). The C-M plot (Fig. 11c) shows that the grain-size samples were distributed in the transitional area between uniform and pelagic suspension, consistently below the C_U line. The C_U boundary reflected the upper grain-size limit for uniform suspension and represented the maximum hydrodynamic energy just above bottom turbulence [48]. These results suggested that the Huangshan Formation was deposited under lower-energy conditions, characterized by finer sediments and a relatively calm depositional environment.

Previous studies have generally identified the Huangshan Formation as a result of fluvio-lacustrine deposition [4,9,10,15,52]. In the Bayan borehole, the Huangshan Formation is noticeably darker in color than the overlying Harbin and Guxiangtun Formations. It displayed clear bedding structures and a vertical grain-size trend that became coarser downward. The grain size was consistently finer than that of the Guxiangtun Formation. Based on lithological ternary diagrams and C–M plot analyses, the Huangshan Formation was interpreted to represent a shallow lacustrine depositional environment.

5.3 Grain-size End-member Analysis

This study employed the Analysize module in MATLAB for grain-size end-member analysis, following the methodology proposed by Song et al. [18] and Wu et al. [53]. The parametric Weibull function was selected to decompose the grain-size data from the Bayan borehole. A fitting quality of $R^2 > 0.8$ and an angular deviation (θ) < 5° indicated satisfactory model performance. Based on these criteria and adhering to the principle of minimizing the number of end-members while ensuring interpretability [54], a three-component model (EM_1, EM_2, and EM_3) was deemed the most appropriate for the Bayan borehole grain-size dataset.

The end-member analysis results (Figs. 12, 13) showed that all the end-member distributions approximate a log-normal pattern, with sorting progressively improving from poor to good. EM_1 had a modal grain size of 6.72 μm, corresponding to fine silt. It exhibited a bimodal grain-size curve with a relatively sharp but lowest-intensity peak. EM_2 with a modal grain size of 21.20 μm fell within the medium silt range and displayed a narrow distribution and a distinct, sharp peak. EM_3, classified as coarse silt, had a modal grain size of 45.60 μm, featuring the sharpest peak and broadest grain-size distribution among the three end-members.

Table 3
Correlation analysis of end-member components, *Mz*, and >63μm components of Bayan borehole.

	EM_1	**EM_2**	**EM_3**	***Mz***	**> 63μm**
EM_1	1				
EM_2	-0.34	1			
EM_3	-0.67	-0.47	1		
Mz	-0.61	-0.36	0.86	1	
> 63μm	-0.54	-0.47	0.88	0.98	1

Loess deposits typically contain fine-grained components derived from three primary sources: (1) direct wind transport and deposition, (2) aggregation-based migration or adherence of fine particles to coarser grains [55], and (3) clay-sized fractions (< 2 μm) produced by weathering and pedogenesis [56]. In the Bayan borehole, the EM_1 component representing fine silt (modal size: 6.72 μm) was minimal. Particles within the 2–16 μm range can remain suspended at high altitudes and be transported over long distances. Based on previous end-member analyses of Huangshan loess [18,53], this grain-size fraction is interpreted as “background dust” [57]. The EM_2 component corresponded to medium silt. Previous studies have shown that particles ranging from 22 to 31 μm can be transported over medium to long distances through suspension [58], whereas particles larger than 63 μm typically result from short-range transport and deposition under high-energy wind conditions [59,60]. The correlation coefficient between EM_2 and the > 63 μm grain-size fraction was − 0.47 (Table 3), indicating a negative relationship and suggesting that EM_2 was not derived from proximal transport. The EM_2 modal value was slightly lower but comparable to that of the Huangshan Loess (27.20 μm), and it is regarded as a proxy for

southwest wind intensity [18,53]. The southwest monsoon is the prevailing wind system during interglacial summers in the Harbin region [61]. Accordingly, EM_2 can serve as a proxy indicator of the summer monsoon intensity in this region [62]. The EM_3 component falling within the coarse silt fraction was finer than the EM_3 identified in desert loess deposits (54.41 μm). It is positively correlated with both M_z (mean grain size) and the > 63 μm fraction (r = 0.86 and 0.88, respectively), indicating a near-source origin. Its sharp peak and well-sorted grain-size curve reflected the limited transport distance and height. According to Prins et al. [63], because components > 40 μm are typically linked to near-source suspension or saltation under strong winter monsoon forcing, EM_3 was interpreted as a proxy for winter monsoon strength in the Bayan region.

5.4 Analysis of Palaeoclimate Evolution

By integrating the comparative curves of magnetic susceptibility, mean grain size, grain-size end-members, and marine oxygen isotope records (Fig. 14), this study investigated climate and environmental changes in the eastern Songnen Plain from the Middle Pleistocene. During this period, magnetic susceptibility values were generally low, mostly below 10×10^{-8} m³/kg. Previous studies on the Songnen Plain have demonstrated that magnetic susceptibility tends to increase during dry and cold periods and decrease during wet and warm intervals [15,53,64–65]. Prior to ~ 250 ka, the EM_3 content exhibited a fluctuating trend, indicating progressive intensification of the East Asian winter monsoon and a shift toward colder and drier climatic conditions in the Harbin region. Conversely, EM_2 displayed an opposing trend, with generally low values, reflecting a weaker summer monsoon. These patterns are consistent with regional paleoclimatic reconstructions [18,53]. Thus, the mid-Middle Pleistocene climate in the eastern Songnen Plain was marked by a strengthening winter monsoon and weakening summer monsoon, indicative of a predominantly cold and arid environment. The variations in the end-member components, M_z, and magnetic susceptibility were closely aligned with glacial-interglacial cycles. During glacial periods, intensified winter monsoons led to elevated EM_3 content, while interglacial periods saw increased EM_2 levels, highlighting the role of global ice volume as a primary control on regional monsoonal dynamics [18]. Notably, at approximately 45 m depth, corresponding to the MIS9 stage, a marked increase in magnetic susceptibility was observed. At this level, curve changes of grain size end-members were highly coupled with M_z. The EM_2 component increased sharply, the EM_3 component significantly decreased, and the mean grain size also increased. This coupled signal reflects a significant glacial-interglacial transition event during the mid-Middle Pleistocene.

After approximately 250 ka, the regional climatic environment of the eastern Songnen Plain underwent a marked transition. The fine-grained EM_2 component exhibited a significant increasing trend, whereas EM_3 remained consistently low, with only minor increases. The combined variation patterns of EM_2 and EM_3, along with generally low magnetic susceptibility values, suggested a gradual intensification of the summer monsoon and a shift toward a cooler and more humid climate between 250 ka and 129 ka. Unlike earlier periods, the variations in grain-size end-members and M_z, as well as magnetic susceptibility, show weaker coupling with glacial-interglacial cycles. This decoupling may be attributed to fluctuations in high-latitude solar radiation, which are known to influence regional climate patterns and monsoon intensities [18,53]. These solar-driven changes have altered the dust source dynamics, contributing to the contraction of the Songnen Sandy Land [17] and reducing the supply of locally derived coarse particles. This observation is consistent with sedimentological evidence, as the grain size parameters (M_z, M_d, and C-M plot) of the Wangkui and Bayan boreholes are generally smaller than those of the Huangshan section [17] (Fig. 8).

At the Middle-Late Pleistocene boundary (26.10 m), the Bayan borehole recorded a pronounced increase in magnetic susceptibility, accompanied by a sharp rise in M_z, a significant decline in the EM_2 component, and a notable increase in EM_3. These changes corresponded to the MIS5d-MIS5e transition, suggesting a brief climatic shift in the eastern Songnen Plain characterized by a weakening summer monsoon and a strengthening winter monsoon, leading to drier and colder conditions. This phase lasted for approximately 14 ka. Subsequently, the magnetic susceptibility values decreased and stabilized at low levels, while the EM_2 values continued to rise and remained elevated, which was indicative of a sustained warm and humid climate [22] and consistent with the last interglacial period of the Late Pleistocene [67]. The black clay layer at 17.8–18.8 m was rich in organic matter and contains well-developed iron–manganese concretions, typically formed under alternating dry-wet and freeze-thaw cycles [68]. Despite a marked decline in magnetic susceptibility, the EM_2 and EM_3 components during this interval exhibited contrasting signals: a weakened summer monsoon and a strengthened winter monsoon. This discrepancy may reflect the overriding influence of high-latitude solar insolation during this period [69–71], suggesting that the eastern Songnen Plain experienced a brief warm-humid interlude within the Last Glacial Period.

During the Last Glacial Period, beginning around 41 ka, notable shifts occurred in the trends of the grain-size end-members, M_z values, and magnetic susceptibility curves. These variations aligned with the global climatic patterns of the Last Glacial Period, particularly in high-latitude regions that experienced progressive cooling, declining sea levels, reduced precipitation, and increased aridity [7,72,73]. The eastern Songnen Plain is situated within the cold-temperate to sub-frigid climatic zone, with mean annual temperatures estimated to be over 6°C lower than present-day values [67]. Magnetic susceptibility increased significantly during this period, exhibiting cyclical fluctuations. The EM_2 component remained at moderate to low levels, with frequent variability, whereas EM_3 showed an opposite trend, oscillating upward, indicating strengthening of the winter monsoon. These results suggested that the eastern Songnen Plain underwent climatic progression from cold and dry to cool semi-humid conditions before reverting to cold and dry conditions during the Late Pleistocene.

With the onset of the Holocene Climatic Optimum, regional temperatures increased, precipitation levels rose, and sea levels began to increase. As a result, the eastern Songnen Plain shifted into a mid-temperate zone, characterized by a warm, semi-humid climate. These favorable environmental

conditions promote extensive pedogenesis, leading to the widespread development of fertile black soils.

6. Conclusions

(1) A detailed magnetostratigraphic column was constructed based on the analysis of OSL, ESR, magnetic susceptibility, and paleomagnetic data from the Bayan borehole. The Bayan borehole record revealed one normal polarity zone (N1) and three geomagnetic excursions (e_1, e_2, and e_3). The N1 zone corresponded to the Brunhes Normal Polarity Chron, while the excursions were correlated with the Iceland Basin, Calabrian Ridge 0, and unnamed geomagnetic excursions, respectively.

(2) Based on the comprehensive analyses of lithology, chronological data, grain-size distribution, and magnetostratigraphic characteristics, the Bayan borehole stratigraphy was divided, from oldest to youngest, into the following units: the Huangshan Formation (35.50–58.00 m), dated to the Middle Pleistocene; the Harbin Formation (18.80–35.50 m), corresponding to the Late Middle Pleistocene to Early Late Pleistocene; the Guxiangtun Formation (1.50–18.80 m), assigned to the Middle to Late Late Pleistocene; and the Holocene Series (0–1.50 m). The depositional environments inferred from the sedimentological evidence indicated that the Huangshan Formation represented shallow lacustrine deposits, the Harbin Formation reflected aeolian sedimentation, and the Guxiangtun Formation corresponded to fluvial deposition.

(3) The grain-size end-member analysis of the Bayan borehole was conducted using the Analysize method, and three effective components were identified. EM_1 (6.72 μm) corresponded to the atmospheric background dust; EM_2 (21.20 μm) reflected the input from more distal sources and served as a proxy for summer monsoon intensity; EM_3 (45.60 μm) indicated proximal material transport, representing the strength of the winter monsoon.

(4) In the eastern Songnen Plain, the Middle Pleistocene climate, marked by a transition boundary around 250 ka, shifted from cold, dry to cool, moist conditions. During the Late Pleistocene, the region experienced climatic evolution from cold-dry to cool-semi-humid, followed by a return to cold-dry conditions. The Holocene was characterized by a warm and semi-humid climate.

Declarations

Declaration of Competing Interest

The work has not been submitted elsewhere for publication, in whole or in part, and all the authors listed have approved the manuscript that is enclosed. No conflict of interest exits in the submission of this manuscript.

Author Contribution

Haonan Song: writing-reviewing and editing. Zhongkai Liang, Mingxin Duan & Muxiao Liu: writing-original draft preparation. Liye Liu, Zhuo Chen, Shoude Han & Haicheng Zhang: data acquisition and processing. Chuanfang Zhou: writing-reviewing and editing.All authors reviewed the manuscript.

Acknowledgement

This research was funded by the funding project of Northeast Geological S&T Innovation Center of China Geological Survey (No.QCJJ2023-30) and Geological survey project of China Geological Survey (No.DD20242507). The authors would like to thank all the reviewers who participated in the review and MJEditor (www.mjeditor.com) for its linguistic assistance during the preparation of this manuscript.

Data Availability

The datasets used and/or analysed during the current study available from the corresponding author on reasonable request.

References

1. Sun, J. Z., Wang, Y. Z. & Zhang, Q. Y. Classification of Quaternary strata in Songliao Plain: Application of several chronological methods. *J. Xi'an Inst. Geol.* **2**, 79-91 (1982).
2. Xia, Y. M., Wang, P. F. & Wang, M. H. Priliminary research on spore-pollen association of the section of Huangshan in Harbin. *Geogr. Sci.* **3**, 183-187 (1983).
3. Ye, Q. X., Wu, J. C., & Wei, Z. Y. The tectonic uplift occurred in Huang Shan in the last thousands of year. *Geogr. Sci.* **4**, 383-388 (1984).

4. Chu, B. J., Gao, Z. C., Yang, S. S. & Xi, X. H. Quaternary magnetostratigraphic classification of the Song-nen Plain (Songhuajiang River-Nenjiang River Plain). *Mar. Geol. Quat. Geol.* **8**, 91-96 (1998).
5. Qiu, S. W., Xia, Y. H., Wang, P. F. & Li, F. H. Study on Pleistocene strata and their sedimentary environment in Songliao Plain. *Sci. China* (Series B) **18**, 431-441 (1988).
6. Xie, Y. Y., He, K. & Kang, C. G. Grain-size distribution of fall-outs of an exceedingly large dust storm in Harbin City and its implications. *Geol. China* **32**, 502-506 (2005).
7. Zeng, L. et al. Magnetostratigraphy of loess in northeastern China and paleoclimatic changes. *Chin. Sci. Bull.* **56**, 2267-2275 (2011).
8. Wang, E. B. Quaternary sedimentary sequences and their environmental significance in Harbin area (Master's Thesis). 35-39 (Jilin University, 2012).
9. Wei, C. Y., Li, C. A., Kang, C. G. & Chang, G. R. Grain-size characteristics and genesis of the Huangshan loess in Songnen Plain area. *Earth Sci.* **40**, 1945-1954 (2015).
10. Zhan, T. et al. Grain size characteristics of Tianhengshan core and their indications for stratigraphic division in the eastern part of the Northeast Plain of China. *J. Geomech.* **24**, 515-521 (2018).
11. Xie, Y. Y. et al. The loess deposits in Northeast China: The linkage of loess accumulation and geomorphic-climatic features at the easternmost edge of the Eurasian loess belt. *J. Asian Earth Sci.* **181**, 103914 (2019).
12. Zhan, T. et al. Magnetostratigraphic dating of a drill core from the Northeast Plain of China: Implications for the evolution of Songnen paleo-lake. *Chin. Sci. Bull.* **64**, 1179-1190 (2019).
13. Zhan, T. et al. Decreasing summer monsoon precipitation during the Mid-Pleistocene transition revealed by a pollen record from lacustrine deposits of the Northeast plain of China. *Palaeogeogr. Palaeoclimatol. Palaeoecol.* **611**, 111357 (2023).
14. Wang, Y., Dong, J. & Yang, J. S. Quaternary stratigraphy of the Huangshan section in Harbin. *Earth Sci.* **45**, 2662-2670 (2020).
15. Wu, P. et al. The genesis of Huangshan loess in Harbin: Integrated evidence from grain size, geochemistry, magnetization, sedimentation and landform. *Acta Geoscientica Sin.* **41**, 420-430 (2020).
16. Liu, S. et al. Evolution of summer monsoon in Songnen Plain since Middle Pleistocene: Magnetic susceptibility, geochemistry and total organic carbon records from Harbin loess. *Chin. J. Geol.* **56**, 1279-1298 (2021).
17. Wu, P. et al. Loess accumulation in Harbin with implications for Late Quaternary aridification in the Songnen Plain, Northeast China. *Palaeogeogr. Palaeoclimatol. Palaeoecol.* **570**, 110365 (2021).
18. Song, Y. et al. Comparative analysis of grain size end member of Harbin loess and climatic significance. *Prog. Geogr.* **42**, 1825-1840 (2023).
19. Song, H. N. et al. Grain-size characteristics and genesis of Bayan loess in the eastern of Songnen Plain. *Chin. J. Geol.* **59**, 1748-1758 (2024).
20. Chen, Y. Y. et al. Quaternary strata lithological characteristics and environmental geological significance of borehole WKZK01 in the eastern Songnen Plain. *J. Geomech.* **30**, 952-964 (2024)
21. Xia, R. et al. Weathering Process of Parent Material and Accumulation Process of Organic Carbon on the Black Soil Profile: A Case Study from the Keshan Area of the Songnen Plain in Northeast China. *Acta Geol. Sin.* **99**, 258-271 (2025).
22. Xia, Y. M. & Wang, P. F. The paleobotany and paleoclimate in the songnen plain: A study on the late tertiary-pleistocene spore pollen assemblages. *Acta Geographica Sin.* **42**, 165-178 (1987).
23. Hou, H. X. et al. Technology and method of the ground substrate layer survey of natural resources: Taking baoding area as an example. *Northwest. Geol.* **54**, 277-288 (2021).
24. Yin, Z. Q., Chen, Z. R., Li, X., Wei, X. F. & Shao, H. Connotation, layering, mapping and supporting objectives of the integrated survey of ground substrates. *Hydrogeol. Eng. Geol.* **50**, 144-151 (2023).
25. Yuan, G. L. et al. Introduction to the methods of ecology-geological survey for servicing ecological civilization: Example from ecology-supporting sphere survey. *Northwest. Geol.* **56**, 30-38 (2023).
26. Hao, A. B. et al. The scientific connotation and theoretical framework of ground substrate. *Acta Geol. Sin.* **98**, 3225-3237 (2024).
27. Yang, K. et al. Ground substrate survey to support black soil conservation and rural revitalization: Taking Hailun city, Heilongjiang province as an example. *Nat. Resour. Inf.* **11**, 9-17 (2024).
28. Editorial Board of Chinese Stratigraphic Code. *Chinese Code of Stratigraphy (Quaternary)*. 96-100 (Geological Publishing House, 2000).
29. Bureau of Geology and Mineral Resources of Heilongjiang Province. *Regional Geology of Heilongjiang Province*. 238-245 (Geological Publishing House, 1993).
30. Zhao, H. Q. et al. Investigation and Evaluation of Groundwater Resources and Environmental Problems in Songnen Plain. (National Geological Data Center, 2007).
31. Folk, R. L. & Ward, W. C. Brazos River bar [Texas]; a study in the significance of grain size parameters. *J. Sediment. Res.* **27**, 3-26 (1957).
32. Kirschvink, J. L. The least-squares line and plane and the analysis of palaeomagnetic data. *Geophys. J. Int.* **62**, 699-718 (1980).
33. Bol'shakov, V. A. Geomagnetic excursions: A reliable means for correlation of geological deposits? *Izv. Phys. Solid Earth* **43**, 773-782 (2007).

34. Laj, C., Kissel, C. & Roberts, A. P. Geomagnetic field behavior during the Iceland basin and Laschamp geomagnetic excursions: A simple transitional field geometry? *Geochem. Geophys. Geosyst.* **7**, Q03004 (2006).
35. Roberts, A. P., Tauxe, L. & Heslop, D. Magnetic paleointensity stratigraphy and high-resolution Quaternary geochronology: Successes and future challenges. *Quat. Sci. Rev.* **61**, 1-16 (2013).
36. Singer, B. S. A Quaternary geomagnetic instability time scale. *Quat. Geochronol.* **21**, 29-52 (2014).
37. Ogg, J. G. Geomagnetic polarity time scale in *Geologic Time Scale 2020* (eds. Gradstein, F. M., Ogg, J. G., Schmitz, M. D. & Ogg, G. M.) 159-192 (Elsevier, 2020).
38. Cohen, K. M., Finney, S. C., Gibbard, P. L. & Fan, J. X. The ICS international chronostratigraphic chart. *Episodes* **36**, 199-204 (2013).
39. Ye, Q. X. The lower boundary of the Guxiangtun formation and its dating. *J. Stratigr.* **14**, 315-320, 260 (1990).
40. Xu X W, Qiang X K, & Zhao Q. Review of the magnetic excursions in Brunhes chron recorded in loess sediments in China. *Progress in Geop.* **31**, 2011-2019(2016).
41. Liu, D. S. *Loess and Environment*. 191-379 (Science Press, 1985).
42. Lu, H. Y. & An, Z. S. Comparison of grain-size distribution of red clay and loess-paleosol deposits in Chinese Loess Plateau. *Acta Sedimentol. Sin.* **17**, 226-232 (1999).
43. Sun, D. H., Lu, H. Y., David, R., Sun, Y. B. & Wu, S. G. Bimode grain-size distribution of Chinese loess and its paleoclimate implication. *Acta Sedimentol. Sin.* **18**, 327-335 (2000).
44. Huang, X. Y., Gao, M. S., Hou, G. H., Zhang, G. & Dang, X. Z. Grain size characteristics and environmental response of marine sediments in Laizhou Bay. *East China Geol.* **44**, 402-414 (2023).
45. Shepard, F. P. Nomenclature based on sand-silt-clay rations. *J. Sediment. Res.* **24**, 151-158 (1954).
46. Link, A. G. Textural classification of sediments. *Sedimentology* **7**, 249-254 (1966).
47. Passage, R. Grain size representation by CM pattern as a geologic tool. *J. Sediment. Res.* **34**, 830-847 (1964).
48. Shaanbei Team of Chengdu Geological College. *Sedimentary Rock Grain Size Analysis and Its Applications*. 66-70 (Geological Publishing House, 1978).
49. Wang, Y. et al. Quaternary sedimentary characteristics and paleochannel evolution in the Anqing valley of the Yangtze River. *East China Geol.* **44**, 300-312 (2023).
50. Qiu, S. W. *Research and Application of Quaternary Geomorphology in Northeast China*. 154-195 (Jilin Science and Technology Press, 2008).
51. Yin, Z. Q., Qin, X. G., Wu, J. S. & Ning, B. The multimodal grain size distribution characteristics of loess, desert, lake and river sediments in some areas of northern China. *Acta Sedimentol. Sin.* **27**, 333-351 (2009).
52. Zhang, X. Q. The differentite on palaeoenvironment of Huang shan area since 100 million years. *Nat. Sci. J. Harbin Normal Univ.* **11**, 90-97 (1995).
53. Wu, P. et al. Provenance variations of the loess deposits in the East Asian monsoon boundary zone, Northeast China: Response to the variations of climate and wind regimes. *CATENA* **222**, 106804 (2023).
54. Bai, M., Lu, R. J., Ding, Z. Y. & Wang, L. D. End Member analysis of grain size in the east of Qinghai Lake and its environmental implications. *Quat. Sci.* **40**, 1203-1215 (2020).
55. Ujvári, G., Kok, J. F., Varga, G. & Kovacs, J. The physics of windblown loess: Implications for grain size proxy interpretations in Quaternary paleoclimate studies. *Earth Sci. Rev.* **154**, 247-278 (2016).
56. Sun, D. H. Supper-fine grain size components in Chinese loess and their palaeoclimatic implication. *Quat. Sci.* **26**, 928-936 (2006).
57. Sun, D. H., Chen, F. H., Bloemendal, J. & Su, R. X. Seasonal variability of modern dust over the Loess Plateau of China. *J. Geophys. Res. Atmos.* **108** (2003).
58. Vriend, M., Prins, M. A., Buylaert, J. P., Vandenberghe, J. & Lu, H. Y. Contrasting dust supply patterns across the north- western Chinese Loess Plateau during the last glacial-interglacial cycle. *Quat. Int.* **240**, 167-180 (2011).
59. Zeng, L. et al. Long- term Pleistocene aridification and possible linkage to high- latitude forcing: New evidence from grain size and magnetic susceptibility proxies from loess- paleosol record in northeastern China. *CATENA* **154**, 21-32 (2017).
60. Li, Y. Reconstruction of monsoonal variations on the northwestern Chinese loess plateau since the late last glacial period. (Northwest Agriculture & Forestry University, 2013).
61. Chen, J. et al. The modulation of westerlies-monsoon interaction on climate over the monsoon boundary zone in East Asia. *Int. J. Climatol.* **41**, E3049-E3064 (2020).
62. Lu, H. Y. et al. Variation of East Asian monsoon precipitation during the past 21 ky and potential CO_2 forcing. *Geology* **41**, 1023-1026 (2013).
63. Prins, M. A. & Vriend, M. Glacial and interglacial eolian dust dispersal patterns across the Chinese Loess Plateau inferred from decomposed Loess grain- size records. *Geochem. Geophys. Geosyst.* **8** (2007).
64. Zhang X R, Ping S F, Jiao Y J. & Liu E H. Characteristics of magnetic susceptibility, grain-size and chromaticity of modern sediments in the southern margin of songnen plain and their paleoclimate environment significance. *J Jinlin University (Earth Science Edition).* **50**, 465-479

(2020).
65. Chen, J. N. et al. Grain sizes characteristics of sediments from QDQ2 borehole in the Yangtze River Delta since the Late Pleistocene and their paleoenvironmental significance. East China Geol. **45**, 466-477 (2024).
66. Lisiecki L E, Raymo M E. A Pliocene-Pleistocene stack of 57 globally distributed benthic $\delta^{18}O$ records. *Paleoceanography*. **20** (2005).
67. Tian, M. Z., Cheng, J. *Quaternary Geology and Geomorphology*. (Geology Press, 2020).
68. Wang, Q. B., Jiang, Z. D. & Sun, Z. X. Distribution and formation environment of Fe-Mn nodules in soils derived from Quaternary loess in North China. *Acta Pedologica Sin.* **56**, 288-297 (2019).
69. Laskar, J. et al. A long-term numerical solution for the insolation quantities of the earth. *Astron. Astrophys.* **428**, 261-285 (2004).
70. Li, Y. et al. Atmospheric dust dynamics over Central Asia: A perspective view from loess deposits. *Gondwana Res.* **109**, 150-165 (2022).
71. Zhang, X. J., Jin, L. Y., Huang, W. & Chen, F. H. Forcing mechanisms of orbital-scale changes in winter rainfall over northwestern China during the Holocene. *The Holocene* **26**, 549-555 (2016).
72. Hu, B. R. & Lu, Y. C. The "silt to clay" ratio, K_d and grain-size cycles of a loess section at Luochan, Shanxi Province. *Acta Petrologica Sin.* **5**, 12-20 (1989).
73. Wang, D. P., Wang, X. K. & Jiang, Y. B. 2010. Reconstruction of the paleo-environment in Changchun area, Northeast China during the Late Mid-Pleistocene: Evidences from sedimentary geochemistry and palynology. *J. Jilin Univ.* **40**, 1066-1074 (2010).

Figures

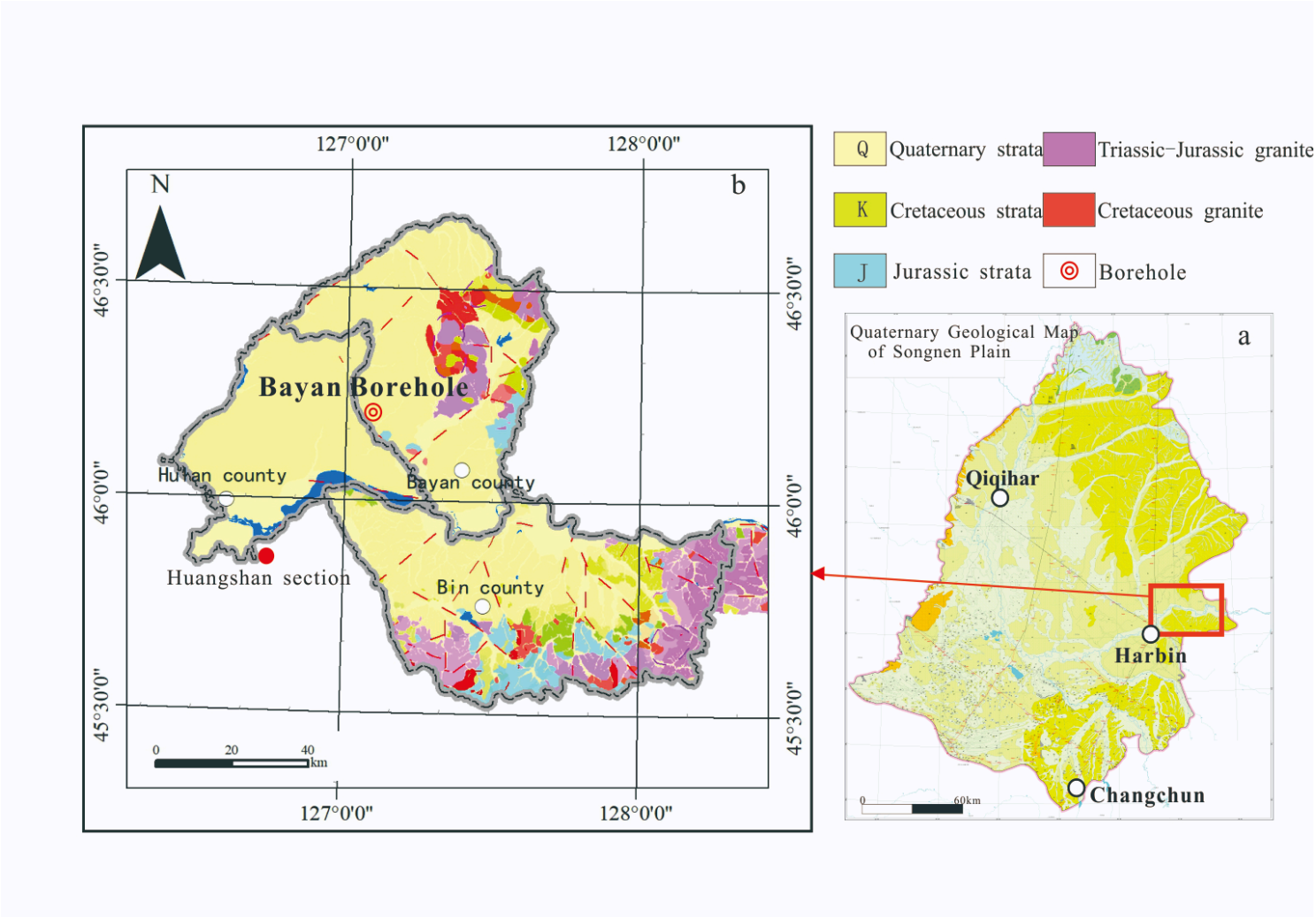

Figure 1

Geological map of Songnen Plain (**a**. modified after [30]) and Bayan borehole location map (**b**).

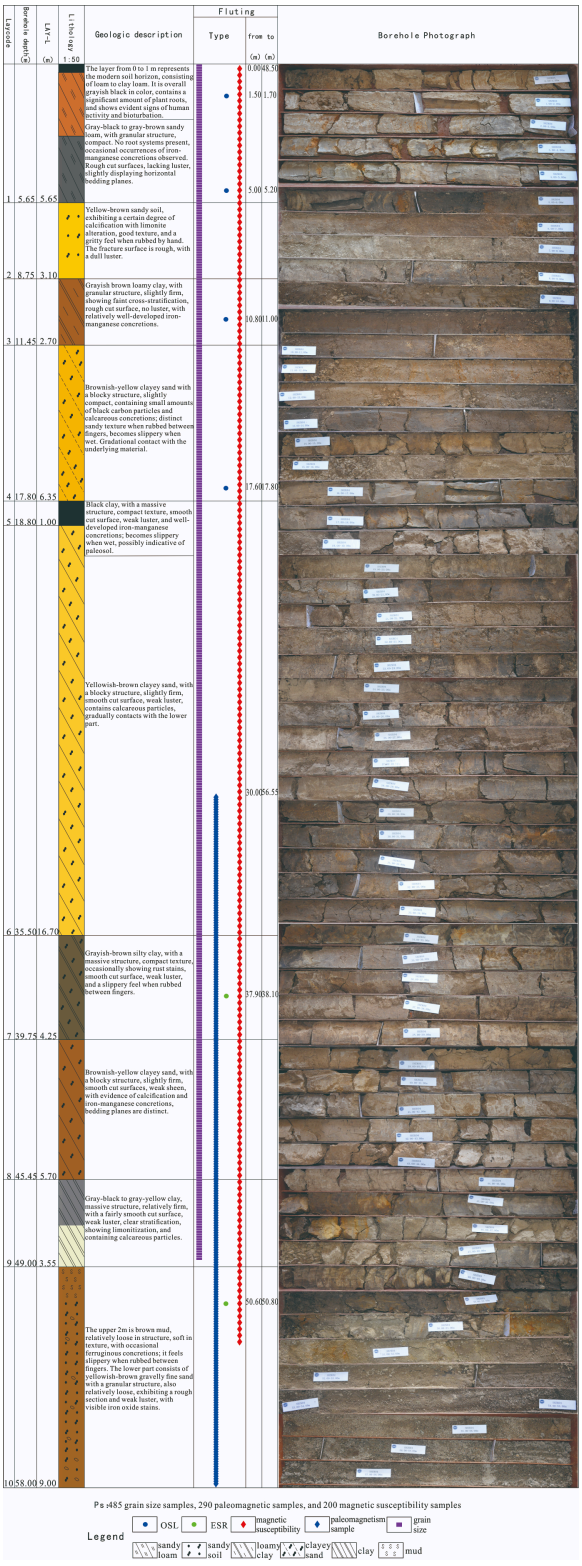

Figure 2

Bayan borehole composite column.

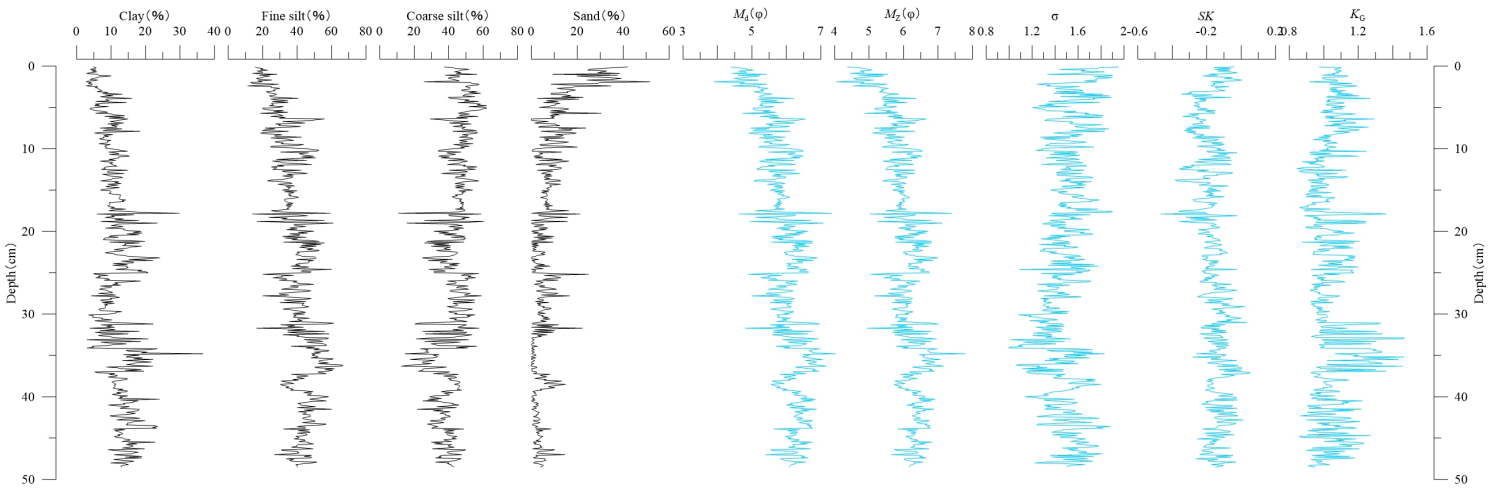

Figure 3

Particle size composition and parameters of Bayan borehole.

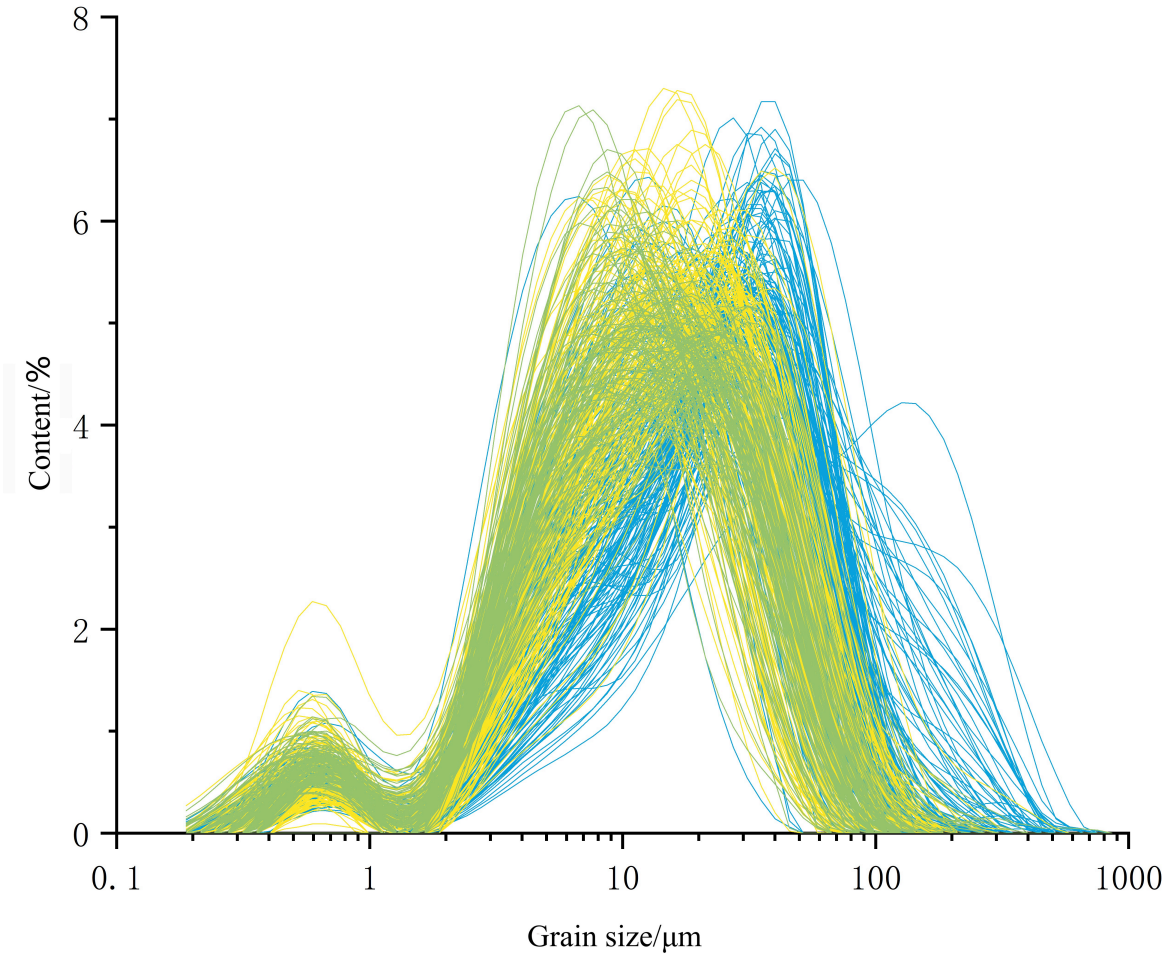

Figure 4

Bayan borehole grain size frequency curves.

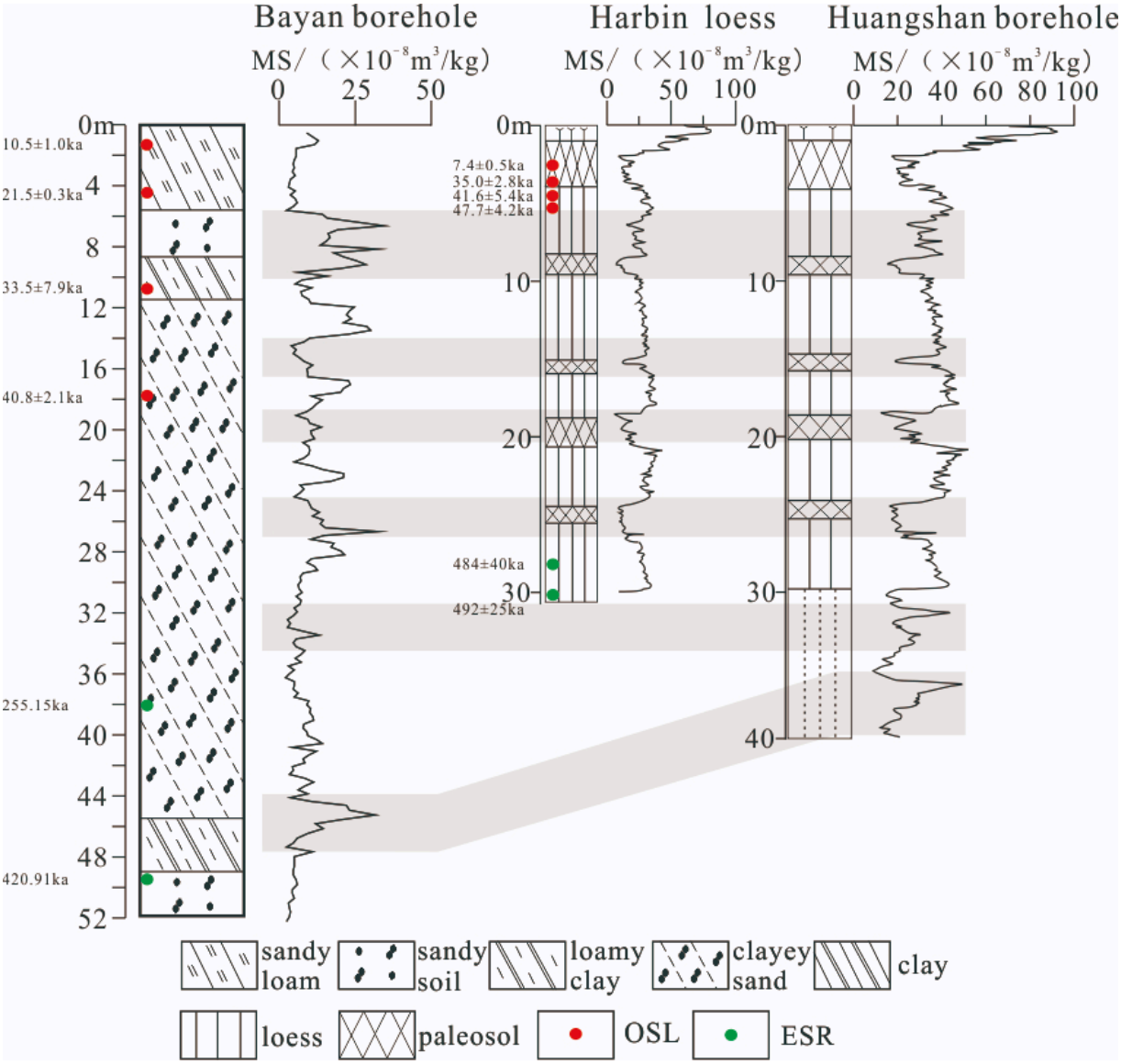

Figure 5

Comparison of magnetic susceptibility between Bayan loess and Harbin loess [16] and Huangshan core [15].

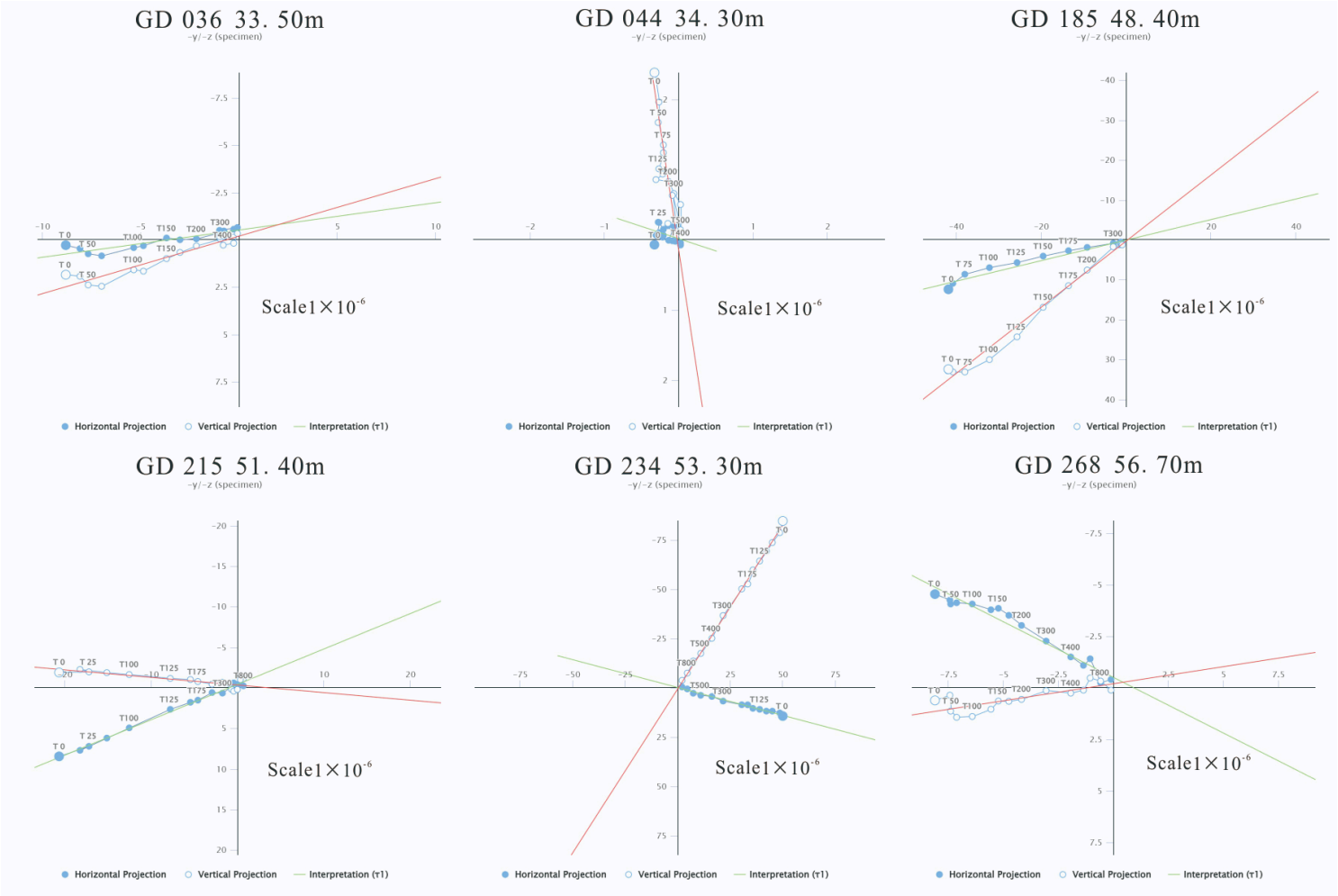

Figure 6

Orthogonal vector projections and intensity plots for AF demagnetization of typical samples. Soild (open) circles represent the projections on the horizontal (vertical) plane. The numbers refer to sample number, depth and AF strength.

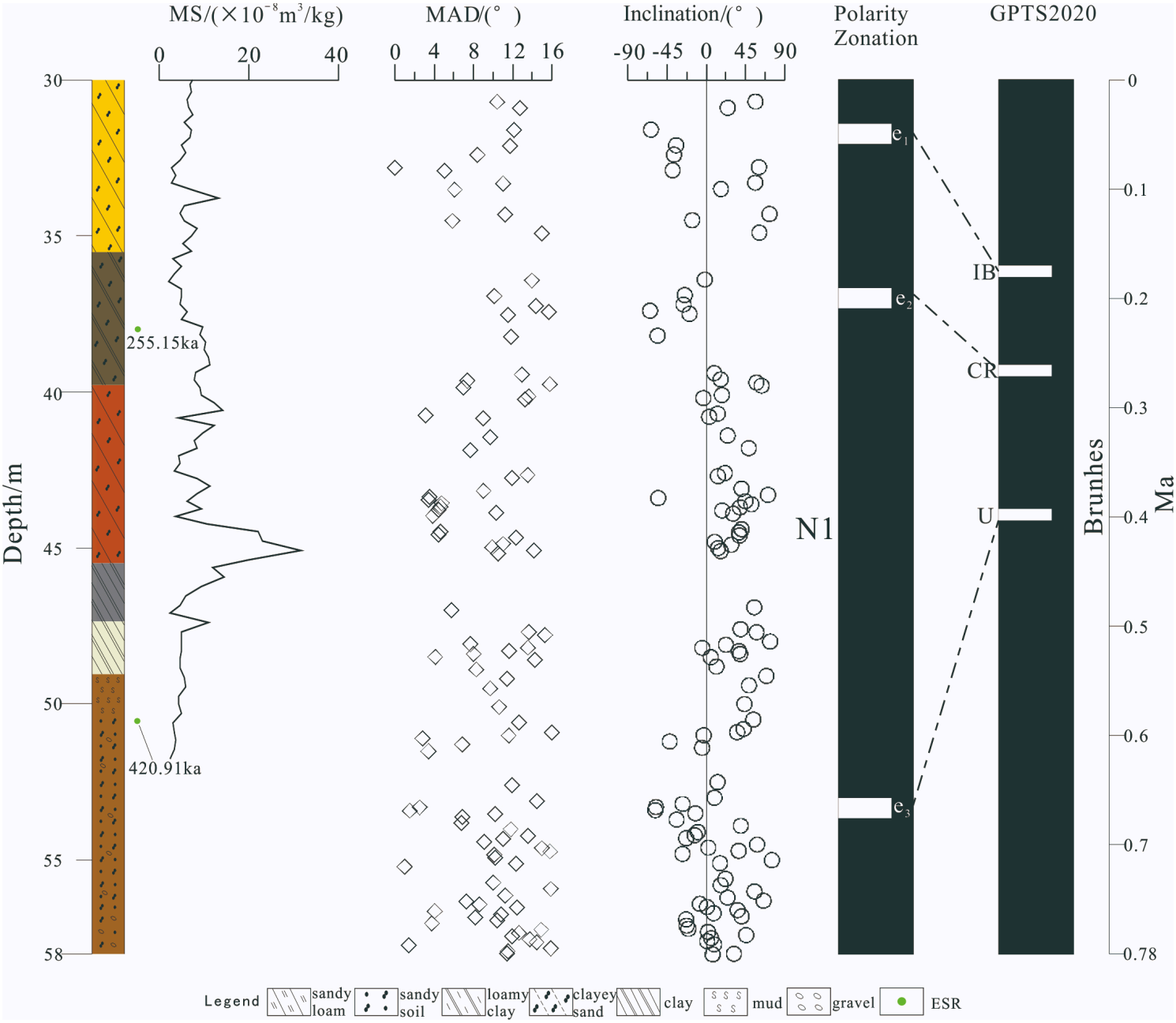

Figure 7

Magnetostratigraphy results of Bayan borehole.

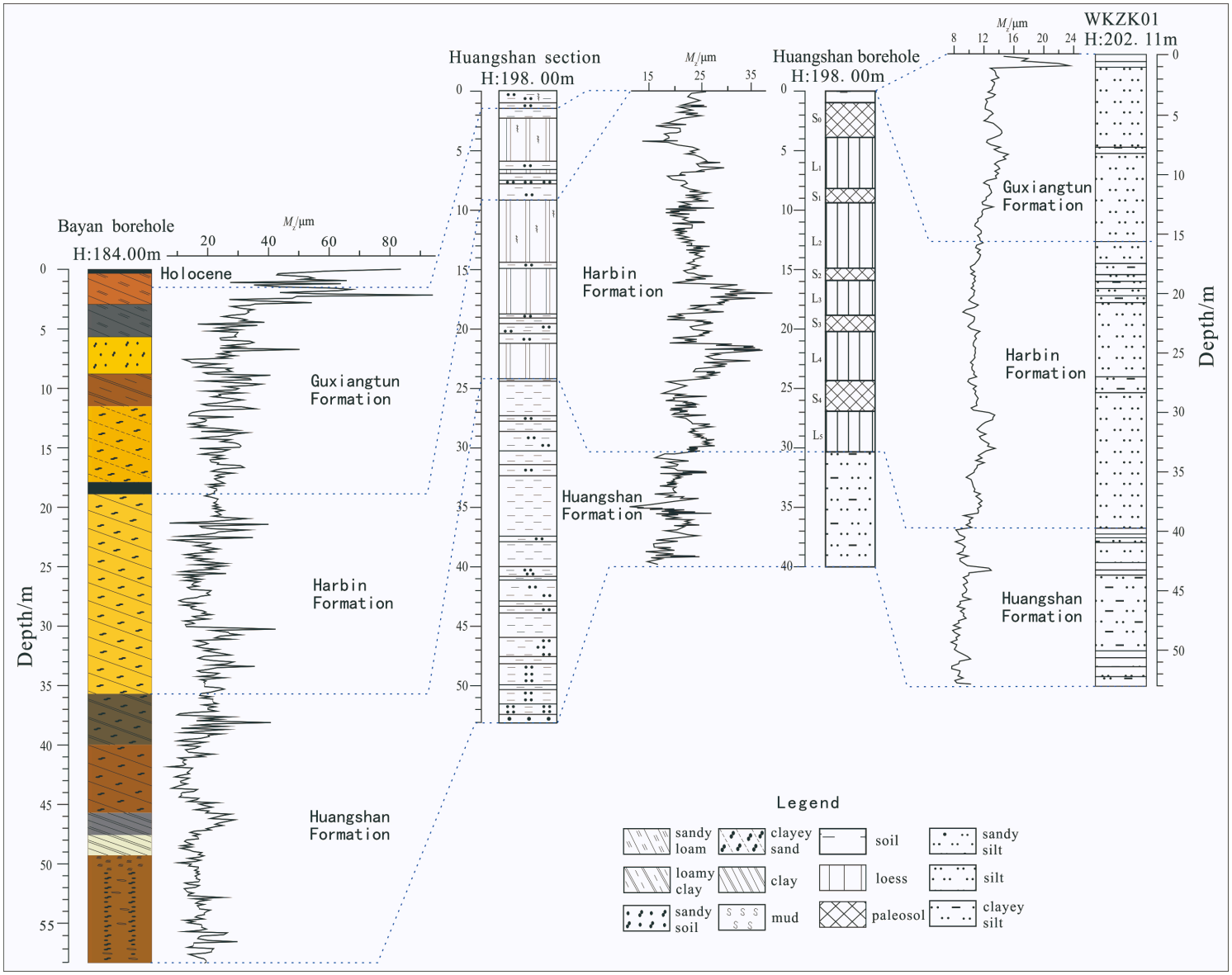

Figure 8

Joint Comparison of Quaternary Strata in the eastern Songnen Plain [14,17,20].

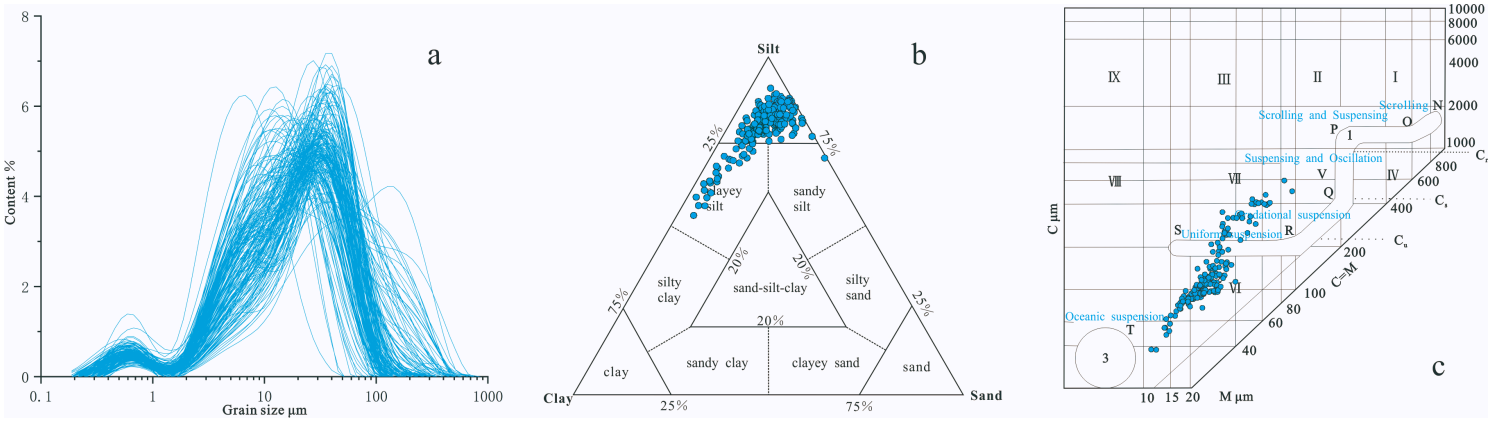

Figure 9

Grain size frequency curves□lithologic triangle map and C-M grain-size map of Guangxiangtun Formation.

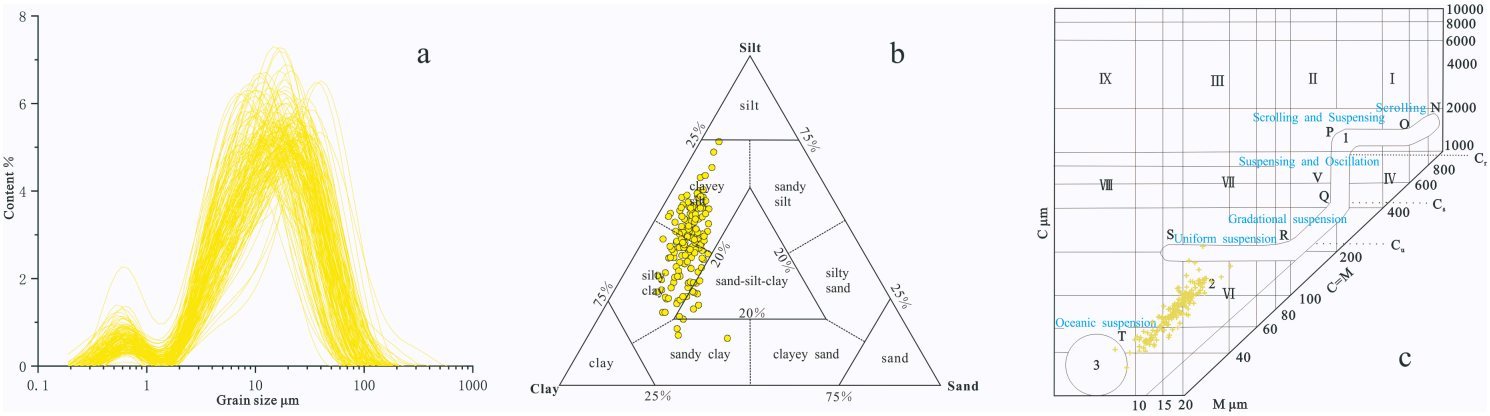

Figure 10

Grain size frequency curves、lithologic triangle map and C-M grain-size map of Harbin Formation.

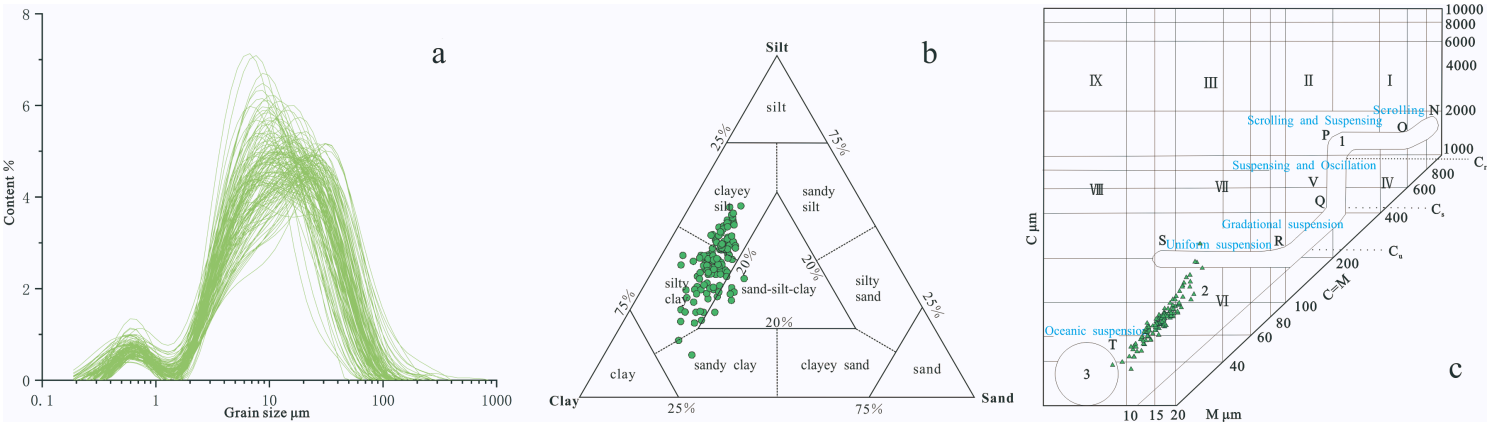

Figure 11

Grain size frequency curves、lithologic triangle map and C-M grain-size map of Huangshan Formation.

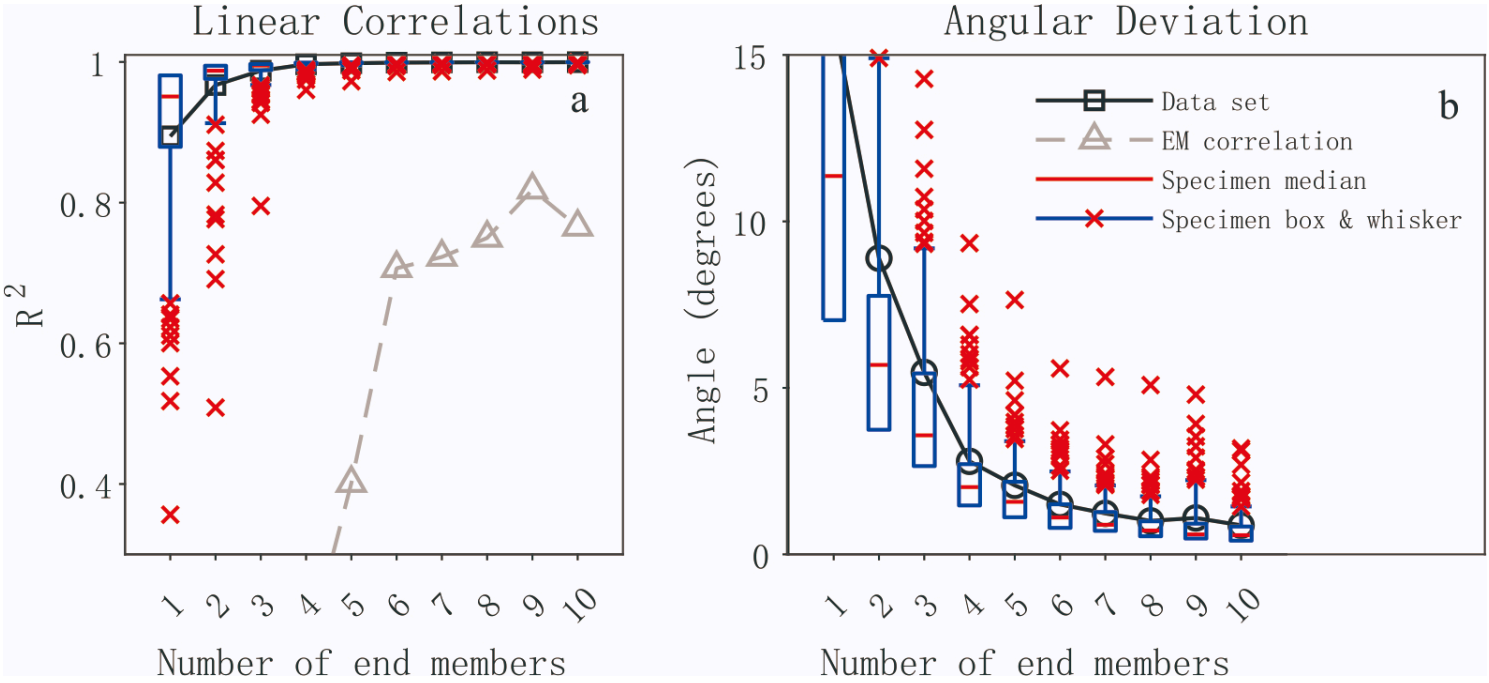

Figure 12

Linear correlation (**a**) and angular deviation (**b**) of end members of Bayan borehole.

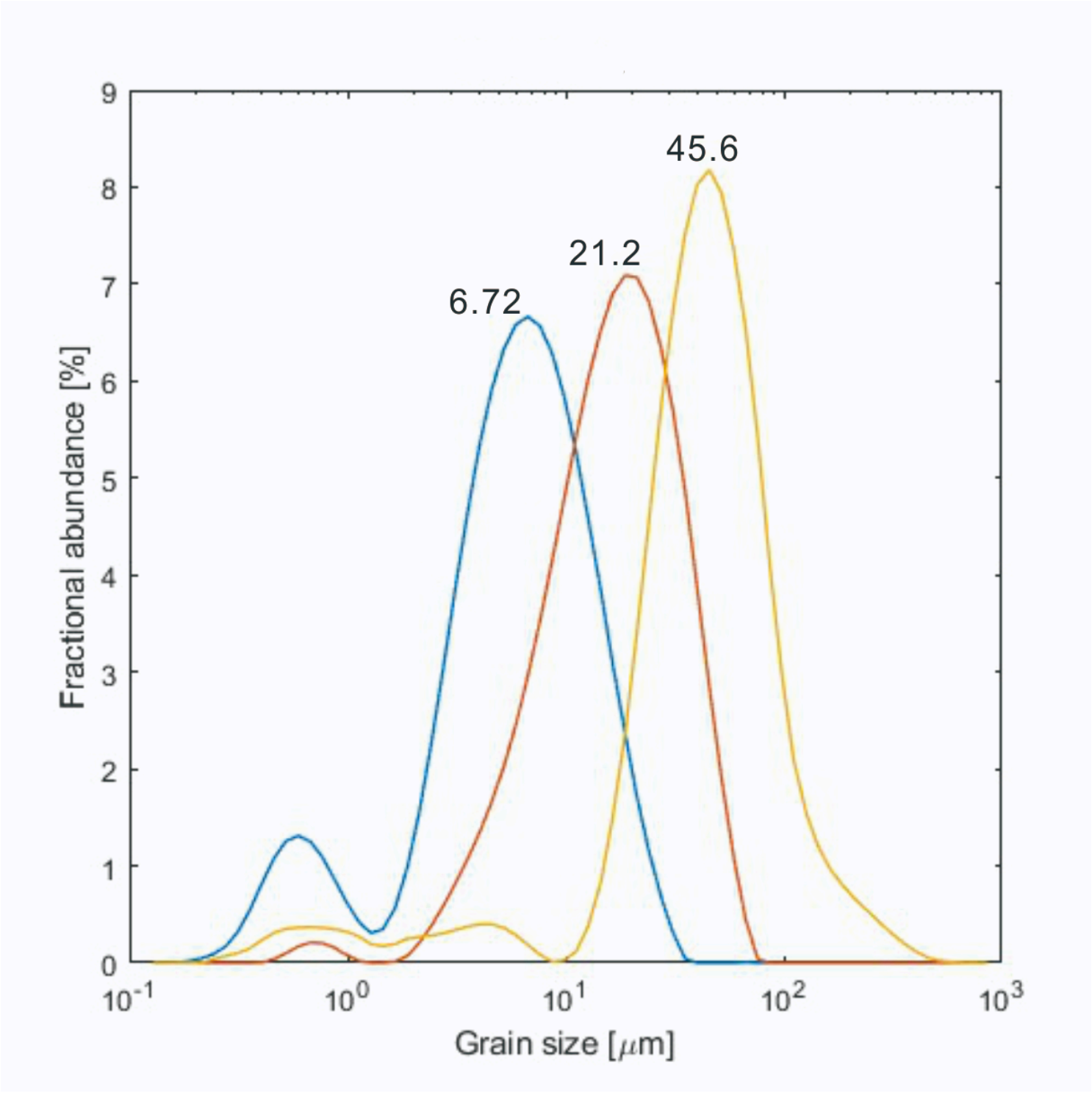

Figure 13

EM_1, EM_2, and EM_3 grain size frequency curves.

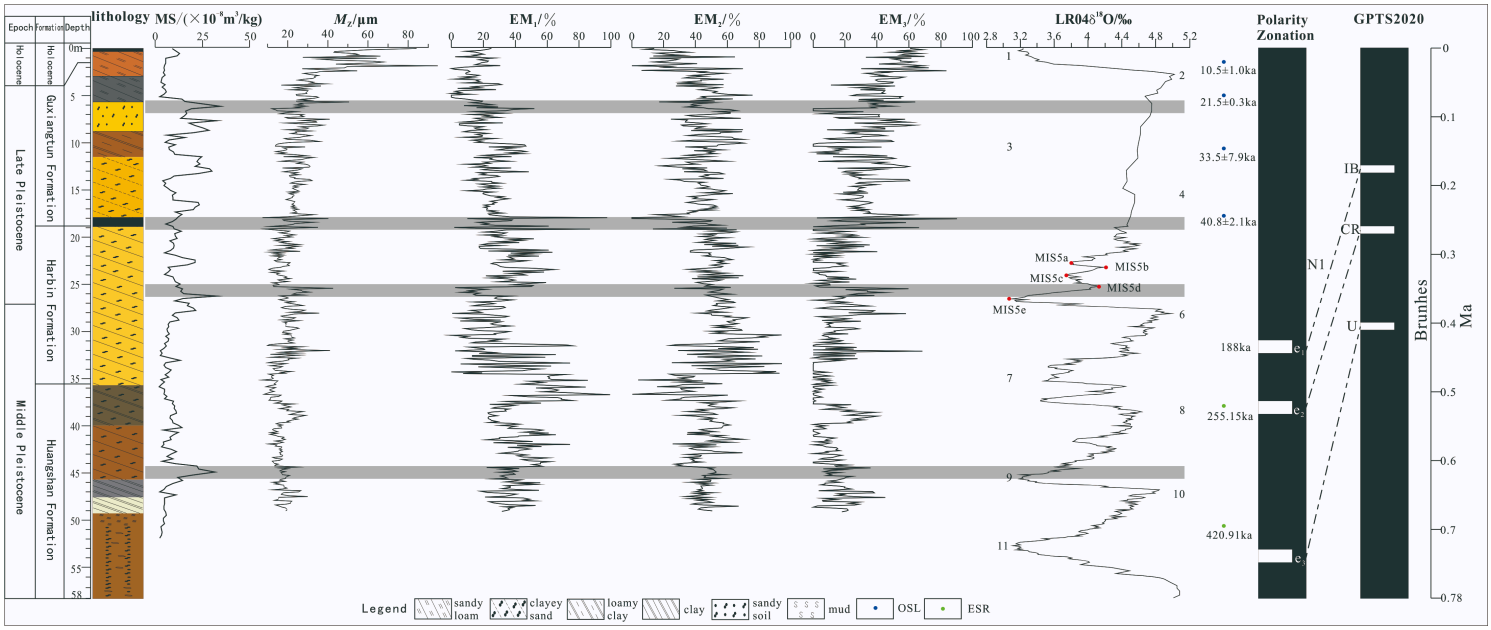

Figure 14

Comprehensive comparison of Grain-size end-members, Magnetic susceptibility, M_Z and LR04$\delta^{18}O$ [66] of the Bayan Borehole.